

## Effects of Spacing between Wind Turbines on Blade Dynamic Stall

A. Choudhry<sup>1</sup>, J. Mo<sup>2</sup>, M. Arjomandi<sup>3</sup> and R. Kelso<sup>4</sup>

<sup>1, 2, 3 and 4</sup> School of Mechanical Engineering  
University of Adelaide, Adelaide, South Australia 5005, Australia

### Abstract

The article presents the results of the application of an analytical model to determine the regions of a tandem wind turbine blade, operating in the wake of an upstream wind turbine, affected by dynamic stall. The wind conditions used as the input for the model were determined based on the Large Eddy Simulation of the turbine wake. The dynamic stall occurrence on the tandem wind turbine blade was studied as a function of the spacing between the wind turbines. It was observed that, even with an ambient turbulence intensity of 0.5% for the upstream wind turbine, approximately 30% of the tandem wind turbine blade was under the influence of dynamic stall for spacing up to at least 20 turbine diameters. The main causes of dynamic stall on the tandem wind turbine blade were shown to be the increased turbulence intensity in the turbine wake and the large rate of change of yaw angle experienced by the tandem wind turbine operating in the wake of the upstream turbine.

### Introduction

Wind turbines generally operate in large groups, known as wind farms, in order to take benefit from geographically limited wind resources and to reduce the overall cost of operation due to the concentration of maintenance equipment and spare parts on the site [4]. However, since most wind turbines operate in the wakes of other wind turbines, following drawbacks associated with this arrangement cannot be over-looked:

- 1) The large increase in turbulence intensity in the wake of a wind turbine results in the increase of unsteady loads on the tandem wind turbines and, hence, reduction of the turbine lifetime.
- 2) The decrease in wind speed caused by energy extraction by the upstream wind turbine results in reduced power production by downstream wind turbines.

The wind farm optimal layout needs to cater for both of the above issues. However, due to the constraints associated with the available land, wind farms are generally designed to yield maximum power output and little regard is given to the increased turbulence intensity.

A major unsteady load on wind turbines is dynamic stall, caused when the static stall angle of an airfoil is suddenly exceeded which results in large increase in lift [8]. The delay in flow separation as the static stall angle is surpassed results in the formation of a large leading edge vortex generally termed as the dynamic stall vortex. However, as the vortex sheds downstream, the airfoil goes into a state of deep stall. The steep decrease in the lift force due to dynamic stall is more severe compared to its static counterpart. This phenomenon results in large unsteady loads on the wind turbine blades as well as performance losses.

Dynamic stall in wind turbines can be caused by unsteady inflow, yaw misalignment, tower shadow and wind gusts. All these

factors contribute in the rapid variations of the turbine blade angle of attack, which in turn results in dynamic stall. For the case of tandem positioning of turbines, the 30-50 times increase in turbulence intensity in the wake is considered to be the most important cause of dynamic stall on tandem wind turbine blades.

In the current article, a previously developed analytical model [1] is used to predict the threshold radius for a downstream wind turbine blade as a function of spacing between the turbines. The threshold radius is defined as the percentage of the blade span beyond which the probability of dynamic stall occurrence falls to zero. The predictive model employs the oncoming wind conditions as inputs and, based on these, calculates the regions of the wind turbine blade affected by dynamic stall. This is accomplished by determining the distribution of reduced frequency on the wind turbine blade, which is then compared with the limiting reduced frequency. Limiting reduced frequency is defined as the minimum reduced frequency or the pitch rate at which the most salient features of dynamic stall become evident. These features include the formation of the dynamic stall vortex on the airfoil suction side and the hysteresis in the forces with angle of attack. The regions where the calculated reduced frequency is larger than the limiting reduced frequency for a particular azimuth angle are the dynamic-stall-affected regions. These are the regions where the ambient wind conditions are severe enough to result in dynamic variations of blade angle of attack to cause dynamic stall.

In this article, Large Eddy Simulation (LES) was used to obtain the wake characteristics behind a wind turbine. The LES results therefore provided the operating environment for the downstream wind turbine. The predictive model was employed to study the distribution of threshold radius as a function of spacing between the wind turbines.

### Wake characteristics using Large Eddy Simulation

The wake characteristics downstream of a horizontal axis wind turbine operating inside a “numerical” wind tunnel were determined using LES [6]. The schematic of the computational domain is shown in Fig. 1. The simulation was performed on the NREL Phase VI wind turbine that was tested inside the NASA Ames 24.4m by 36.6m wind tunnel. The rotor diameter ( $d$ ) of the turbine is 10.1m and the turbine is rotating at an rpm of 71.6. The simulation was performed with a constant inflow velocity of 7m/s, inflow turbulence intensity of 0.2% and a yaw angle of zero degrees as shown in Fig. 1. LES results were validated by comparing the chord-wise pressure coefficients at the selected span-wise stations with the experimental results [2, 8] and a very good agreement was observed between the two.

In this section, the wake characteristics behind the wind turbine are presented for quick reference. Note that the total simulation time was 8.3448s, corresponding to ten revolutions of the turbine blades. The space- and time-averaged axial velocity, axial turbulence intensity, yaw angle and the rate of change of yaw angle (experienced by the tandem wind turbine) as a function of

normalized downstream distance ( $y/d$ ) are presented. It is important to note that the rotational axis of the tandem wind turbine is assumed to be aligned with the rotational axis of the upstream wind turbine.

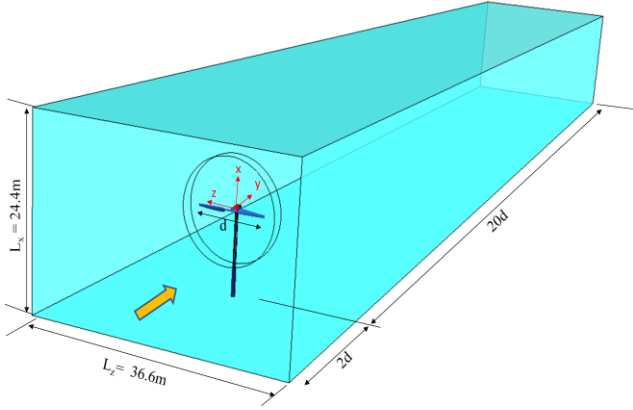


Figure 1. Schematic illustration of the computational domain for LES used in analysis of the wake characteristics behind a wind turbine in a numerical wind tunnel.

### Velocity Deficit and Turbulence Intensity in the Wake

The space- and time-averaged axial velocities normalized by the upstream wind speed ( $V_W$ ) of 7m/s and the local axial turbulence intensity in the wake of the upstream wind turbine are plotted as a function of normalized downstream distance ( $y/d$ ) in Fig. 2. The local turbulence intensity  $(I_{wake})_i$  in the axial direction is given by the following expression:

$$(I_{wake})_i = \frac{\sqrt{(v'^2)_i}}{V_{y_i}}$$

In the above equation, the subscript  $i'$  represents the corresponding  $y/d$  location in the wake of the upstream wind turbine,  $V_{y_i}$  is the mean axial velocity and  $\sqrt{(v'^2)_i}$  indicates the fluctuations in the axial wind speed at the same  $i^{th}$  station.

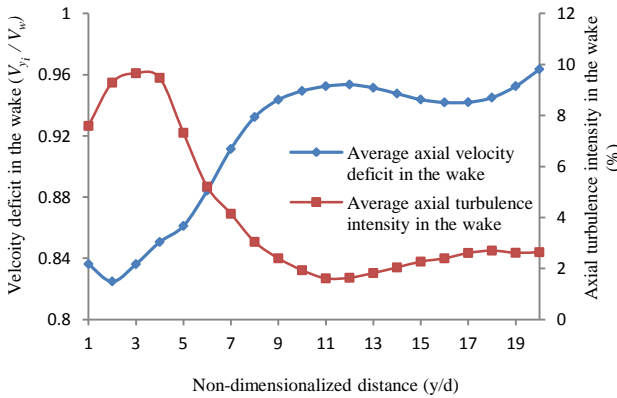


Figure 2. Space- and time-averaged axial velocity deficits, normalized by the inflow velocity, and the local axial turbulence intensity in the wake of a wind turbine as a function of normalized downstream distance.

The energy extraction due to the upstream wind turbine is apparent from the velocity deficit immediately behind the turbine as illustrated in Fig. 2. It can be observed that as the downstream distance increases, the velocity deficit starts to recover. This is due the turbulence in the wake which acts as an efficient mixer. Using the velocity deficits, the mean wind speed at each downstream station were calculated and used as the input to the analytical model.

Furthermore, the large increase in turbulence intensity in the wake is evident as well from Fig. 2. It can be observed that up to  $y/d = 4$ , the turbulence intensities increase and then begin to decay as the distance in the wake is increased. This region was termed as the near-wake region of the wake in reference [6] and is the location at which the large spiral vortex collapses into two pairs of counter-rotating vortices. An interesting phenomenon that can be observed from Fig. 2 is the increase in the turbulence intensity in the far-wake regions (after  $y/d = 11$ ). This increase in turbulence intensity can be attributed to the counter-rotating vortex pairs which have reached the walls of the tunnel. These vortices induce the flow at the extremities of the numerical wind tunnel and therefore result in the increase in the overall turbulence intensity of the system at these stations. Note that the standard deviation (derivative from turbulence intensity) is taken as the measure of the rate of change of wind speed (model input), as proposed by Melbourne [5].

### Wind Direction Parameters in the Wake

In general, the yaw angle and the rate of change of yaw angle for the tandem wind turbine are overlooked when wake characteristics of wind turbines are presented. In the following, assuming that the rotational axis of the tandem wind turbine rotor is aligned with the rotational axis of the upstream wind turbine, the yaw misalignment of the tandem wind turbine has been calculated using the mean velocities in the axial and lateral directions at each downstream station by the following expression:

$$\gamma_i = \tan^{-1} \left( \frac{V_{z_i}}{V_{y_i}} \right)$$

In this equation,  $V_{z_i}$  and  $V_{y_i}$  are the lateral and the axial velocities at the  $i^{th}$  station, respectively. The mean yaw misalignment for the tandem wind turbine is shown in Fig. 3. It can be observed that the mean yaw angle for the tandem wind turbine is approximately zero degrees and therefore the primary wind direction does not vary considerably as compared to the upstream wind turbine.

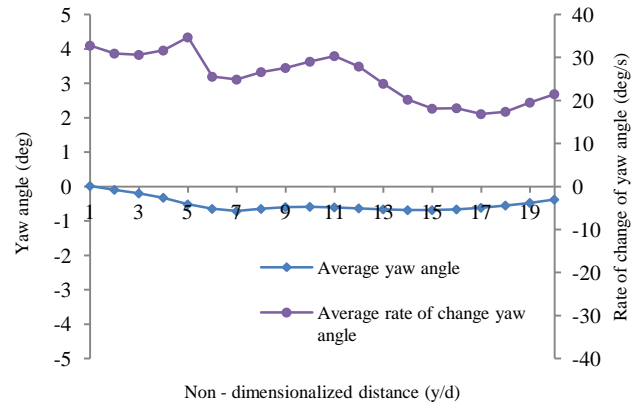


Figure 3. Variation of yaw angle and rate of change of yaw angle, experienced by the tandem wind turbine as a function of normalized downstream distance.

Similarly, the RMS of  $\gamma_i$  has been calculated using the fluctuations in the wind speed in axial and lateral direction at each downstream station according to:

$$rms(\gamma_i) = \tan^{-1} \left( \frac{\sqrt{(\omega'^2)_i}}{\sqrt{(v'^2)_i}} \right)$$

In the above equation,  $\sqrt{(\omega'^2)_i}$  is the fluctuation in the lateral wind speed component and  $\sqrt{(v'^2)_i}$  is the fluctuation in the axial wind speed component at the  $i^{th}$  station. Similar to the rate of

change of wind speed, the rate of change of yaw angle in the wake of a wind turbine is taken to be the RMS or the standard deviation of  $\gamma_i$ . Therefore, for the tandem wind turbine, the rate of change of yaw angle can be given by the RMS of the yaw angle at each station, i.e.  $(\dot{\gamma})_i = (rms(\gamma_i) \text{ per sec})$ . The rate of change of yaw angle experienced by the tandem wind turbine is presented as a function of normalized downstream distance in Fig. 3. It can be clearly observed that, even though the mean yaw misalignment is close to zero, the rate of change of yaw angle for the tandem wind turbine is considerably large. The large rate of change of yaw angle (20-40  $^{\circ}/\text{sec}$ ) is primarily due to the large increase in the turbulence intensity in the wake. Therefore, the parameter cannot simply be ignored when calculating fatigue loads on tandem wind turbine blades. Furthermore, it can be observed that the rate of change of yaw angle decreases with the downstream distance due to a decrease in the turbulence intensity.

In general, the wake characteristics behind the turbine, such as the axial velocities and the turbulence intensities, are determined using empirical relations, such as those presented by [7] and [3]. However, no such empirical relations exist for the wind direction parameters and these are generally ignored when calculating fatigue load of tandem wind turbines.

### Dynamic Stall on Tandem Wind Turbine Blade

In the following, the distribution of threshold radius with respect to the azimuth angle for the upstream and the tandem wind turbine at selected downstream stations ( $y/d = 2, 5, 10, 15$ ) is presented. Note that in the present research, the threshold radius

is calculated using the standard deviation as the rate of change of a parameter with respect to time. This implies that the results presented here are for an averaged case and the threshold radius observed will be the most prevalent value.

The upstream and the tandem wind turbines are similar to the NREL Phase VI wind turbine, both having a rotor diameter of 10.1 m and operating at a constant rotational speed of 71.6 rpm. Furthermore, the vertical wind shear is assumed to be zero for both the upstream and the tandem wind turbine. This implies that the velocity is constant along the entire rotor section for both the upstream and the downstream wind turbines. The blade is composed of the S809 airfoil for which the limiting reduced frequency is 0.026, based on 2D dynamic stall experiments [9]. The rotor of the upstream wind turbine is aligned with oncoming freestream wind and therefore the yaw angle and the rate of change of yaw angle is zero. Furthermore, the rotor of the downstream wind turbine is aligned with the rotor of the upstream wind turbine. The wake of the upstream wind turbine forms the operating environment of the tandem wind turbine. Therefore, the wind conditions experienced by the tandem wind turbine at a selected downstream station are those presented in Fig. 2 and Fig. 3 for the corresponding station.

Based on the aforementioned conditions, the distribution of the threshold radius at selected downstream stations is presented in Fig. 4. The corresponding wind conditions at each station along with the largest threshold radius, identified by  $r_{th_{max}}$ , are also shown. Note that the turbines are rotating in a clock-wise direction.

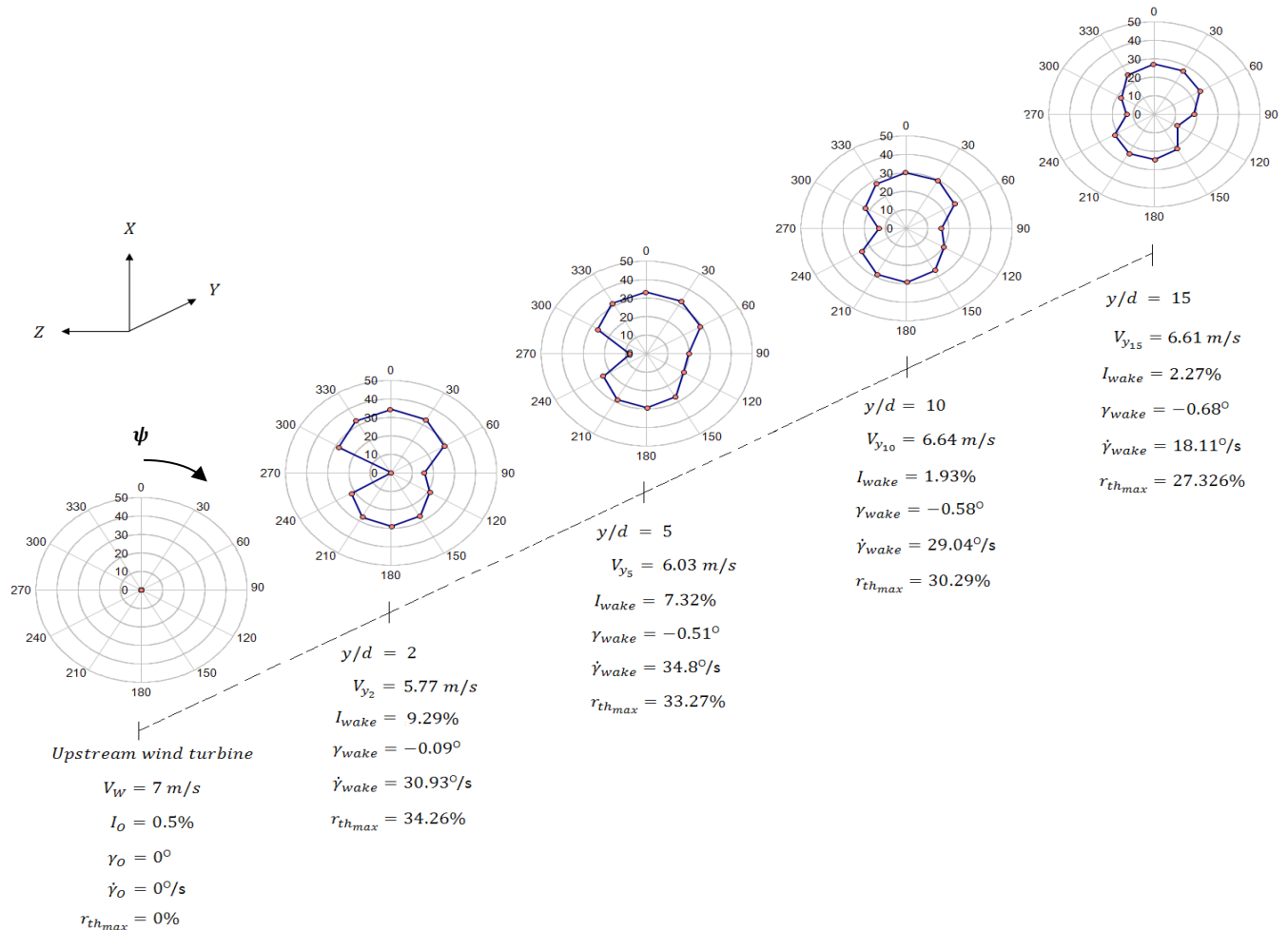


Figure 4. Threshold radius distribution for the upstream and the tandem wind turbine, at selected downstream stations. The corresponding wind conditions at each station, derived from Fig. 2 and Fig. 3, are also shown along with the maximum threshold radius that is observed.

It can be observed from Fig. 4 that, due to very small turbulence intensity and no yaw-misalignment, the threshold radius observed for the upstream wind turbine is zero. This simply implies that, based on the upstream wind conditions, the wind turbine is primarily free of dynamic stall. However, in the wake, an immediate increase of turbulence and a large rate of change of yaw angle result in a larger probability of dynamic stall occurrence. Therefore, for the downstream wind turbines, at all selected downstream stations, a completely asymmetrical-twin-lobe distribution of threshold radius is observed.

It can be observed from Fig. 4 that at  $y/d = 2$ , approximately 34.26% of the tandem wind turbine blade will be affected by dynamic stall. This shows that for the tandem wind turbine, located two rotor diameters downstream of an upstream wind turbine, dynamic stall will be observed at approximately 34.26% of the blade span. Moreover, note that as the distance between the turbines is increased, the maximum threshold radius observed decreases in magnitude, but only slightly. Therefore if the tandem wind turbine is placed fifteen rotor diameters ( $y/d = 15$ ) downstream of the upstream wind turbine, then, due to the smaller turbulence intensity and smaller rate of change of yaw angle, the maximum threshold radius observed during the rotation is 27.326% approximately. Nevertheless, even though the turbulence intensity at this station is comparatively very small (a little over 2%), the maximum threshold radius observed is still significant, primarily due to the large rate of change of yaw angle.

## Conclusion

The purpose of the current research was to calculate the regions of a tandem wind turbine blade, operating in the wake of an upstream wind turbine, susceptible to dynamic stall at selected downstream stations using a predictive model. Large Eddy Simulation was used to obtain the wake characteristics of the NREL Phase VI wind turbine operating in a numerical wind tunnel, with test sections similar to the NASA Ames wind tunnel. The wake characteristics behind the upstream wind turbine served as the model input for the downstream wind turbine.

It was shown that, due to very small turbulence intensity, no dynamic stall event is encountered by the upstream wind turbine. However for the downstream wind turbine, regardless of the downstream station, approximately more than one-fourth of the blade span will be affected by dynamic stall. This, in the near-wake, is caused by the combined effect of large turbulence intensity and large rate of change of yaw angle. However, in the far-wake region, it was observed that the turbulence intensity is considerably smaller but the rate of change of yaw angle is still large. This causes an insignificant change in the threshold radius as the distance behind the turbine is increased. Therefore, it can be concluded that the primary cause of dynamic stall on wind turbines, operating in the wake of upstream wind turbines, are the large yaw rates and the large increase in turbulence intensity in the wake.

## References

- [1] Choudhry, A., Arjomandi, M. and Kelso, R. Horizontal Axis Wind Turbine Dynamic Stall Predictions based on Wind Speed and Direction Variability (Under Review), *Proceedings of the Institution of Mechanical Engineers, Part A, Journal of Power and Energy*, 2012
- [2] Hand, M. & Simms D., *Unsteady Aerodynamics Experiment*, National Renewable Energy Laboratory, 2001.
- [3] Hassan, U., *A Wind Tunnel Investigation of the Wake Structure within Small Wind Turbine Farms*, Harwell Laboratory, Energy Technology Support Unit, 1993.

- [4] Manwell, J.F., McGowan, J.G. and Rogers A.L., *Wind Energy: Explained*, Wiley Online Library, 2002.
- [5] Melbourne, W., Criteria for Environmental Wind Conditions, *Journal of Wind Engineering and Industrial Aerodynamics*, 1978. 3(2-3): p. 241-249.
- [6] Mo, J., Choudhry, A. and Arjomandi, M., Large Eddy Simulation of the Wind Turbine Wake Characteristics in the Numerical Wind Tunnel Model (Under Review), *Journal of Wind Engineering and Industrial Aerodynamics*, 2012.
- [7] Mortensen, N.G., Heathfield, D.N., Myllerup, L., Landberg, L., Rathmann, O., Troen, I. and Petersen, E.L., *Getting Started With WAsP8*, Risø National Laboratory, 2003.
- [8] Simms, D.A., NREL Unsteady Aerodynamics Experiment in the NASA-Ames Wind Tunnel: A Comparison of Predictions to Measurements, National Renewable Energy Laboratory, 2001.
- [9] Ramsay, R.R., Hoffmann, M.J., and Gregorek, G. M., "Effects of Grit Roughness and Pitch Oscillations on the S809 Airfoil", NREL/TP-442-7817, National Renewable Energy Laboratory, Golden, CO, 1995.